Binding of Memantine to Melanin: Influence of Type of Melanin and Characteristics

Martin J. Koeberle,[1] Patrick M. Hughes,[2] Graham G. Skellern,[1] and Clive G. Wilson[1,3]

Received June 10, 2003; accepted June 30, 2003

Purpose. The objectives of this study were to characterize sepia, synthetic, and bovine melanin and to determine their binding characteristics to the drug memantine.

Methods. Physical methods were used to characterize sepia, synthetic, and bovine melanin. Their binding properties toward memantine were determined in deionized water and phosphate-buffered saline (PBS) at 37°C. Melanin–memantine binding was measured indirectly by determining the unbound fraction of memantine. Curve fitting according to the Langmuir binding isotherm for one binding site was used for the determination of binding capacity (B_{Lmax}) and dissociation constant (K_D).

Results. Synthetic and sepia melanin had comparable Gaussian particle size distributions, whereas bovine melanin showed a heterogeneous distribution profile. The suspension medium had a small effect on the particle size distribution of synthetic and bovine melanin. There were characteristic differences in the infrared spectra of the melanins. The rank order for B_{Lmax} in deionized water was sepia > bovine > synthetic melanin. However, when the melanins were suspended in PBS, the B_{Lmax} values were lower, and the rank order was bovine > sepia > synthetic. Whereas the K_D values for sepia and synthetic melanin remained largely the same in deionized water and PBS, the K_D value for bovine melanin in PBS was more than twice than in deionized water.

Conclusions. This study showed that the physical characteristics of the melanins investigated differ markedly. The binding of memantine to melanin is thought to be determined by the different chemistries of the melanins, particle size, and buffer electrolytes.

KEY WORDS: memantine; melanin binding; binding parameters; particle size distribution; infrared spectra.

INTRODUCTION

Melanins, a group of natural pigments of various colors, occur in humans, animals and plants. The black to brown eumelanin and the yellow to red pheomelanin are the two distinct types of melanin found in man. Besides skin, hair, inner ear, and brain, the eye contains the largest amount of pigment (1,2).

In the visual system melanin enhances the optical efficiency by absorbing scattered light and protecting the retina from overexposure (2–4). In the retinal pigmented epithelium (RPE) it has been shown that melanin granules are connected to lysosomal pathways (5). Furthermore, melanin is an effective electron acceptor and hence acts as a radical scavenger and antioxidant (6).

The basic building block of eumelanin is the amino acid tyrosine, which is enzymically converted into the pigment via the precursor 5,6–dihydroxyindole (DHI) or 5,6–dihydroxyindole–2–carboxylic acid (DHICA). Although it is possible to produce synthetically pure DHI- and DHICA-derived melanin, natural eumelanin is a copolymer, and the ratio of DHI to DHICA can show considerable variations leading to complex and random polymers (7–11). During their biosynthesis natural melanins become covalently bonded to proteins, producing an extremely insoluble material (12). Furthermore, the native pigment contains amounts of water that are thought to be vital in maintaining the structure of melanin in a hydrated state (2).

Despite an ongoing discussion about the chemistry and particle character of eumelanin, recent evidence indicates that melanin is an aggregate in nature (7,8,11,13–15). At the molecular level the basic building block is a small planar oligomer comprising about five DHI/DHICA units, which can be in different oxidation states. A stack of three to seven of these oligomers align themselves through noncovalent interactions to form a fundamental aggregate. These primary aggregates are then able to grow into secondary aggregates and even larger agglomerates. Although synthetic melanin is built of DHI/DHICA-derived units as is natural melanin, it is thought that the secondary aggregation is different because the synthetic material is an amorphous solid (8).

The binding of drugs to melanin may have significant pharmacologic consequences (12,16,17). The accumulation of drugs in melanotic tissues such as the RPE may lead to toxicologic effects in the adjacent retina through increased tissue concentrations, altered photochemical properties of the drug–melanin complex or due to extended drug exposure (1,18); however, the binding of drugs to melanin does not appear to be correlated to ocular toxicity. In addition, binding of specific drugs prevents ocular toxicity (19).

In spite of many investigations into the nature of drug binding to melanin, the exact mechanism of this interaction remains unknown. Of the drugs with known melanin affinity, many are positively charged at physiologic pH, and it is generally accepted that ionic interactions contribute significantly. Other factors that contribute to the reversible binding are the drugs' lipophilicity, van der Waal's forces, and the ability to form charge transfer complexes (1,16,17,20–23).

Whereas *in vitro* studies may reveal an underlying mechanism of interaction and allow the determination of the affinity between melanin and drug, other physiologic issues may predominate. Isolated melanin, when suspended in solution, has a smaller particle size, and intracellular melanin is surrounded by membranes, which hinder accessibility (24). Lipophilic drugs diffuse through these membranes more eas-

[1] Department of Pharmaceutical Sciences, Strathclyde Institute for Biomedical Sciences, University of Strathclyde, Glasgow, UK.
[2] Allergan Inc., Irvine, California, USA.
[3] To whom correspondence should be addressed. (email: c.g.wilson@strath.ac.uk)

ABBREVIATIONS: B_L, Melanin–memantine binding; B_{Lmax}, Maximum binding capacity; DHI, 5,6–Dihydroxyindole; DHICA, 5,6-dihydroxyindole-2-carboxylic acid; FT–IR, Fourier transform infrared; HPLC, high-performance liquid chromatography; K_D, dissociation constant; L, ligand; LC–MS, liquid chromatography–mass spectrometry; Log(P), partition coefficient; N, number of determinations; NMDA, N–methyl-D-aspartate; PBS, phosphate-buffered saline; PIDS, polarization intensity differential scattering; pK_a, dissociation constant; R, receptor; RL, receptor–ligand complex; RPE, retinal pigmented epithelium; SD, standard deviation; SE, standard error.

0724-8741/03/1000-1702/0 © 2003 Plenum Publishing Corporation

ily than less lipophilic ones, and therefore, these membranes may influence the determination of binding parameters despite an otherwise similar binding mechanism (12). However, protein moieties conjugated to natural melanins do not affect the characteristics of drug–melanin interactions, as shown by a comparison of the binding capacities of native and hydrolyzed (protein-free) melanin (25).

Memantine hydrochloride (1-amino-3,5-dimethyladamantane hydrochloride, Fig. 1) has putative neuroprotective properties by blocking the calcium channels activated by N-methyl-D-aspartate (NMDA) receptor stimulation (26). Excessive activation of NMDA receptors is thought to mediate the calcium-dependent neurotoxicity associated with neurodegenerative diseases. Currently, memantine is used for the treatment of Alzheimer's and Parkinson's disease. However, its neuroprotective properties suggest that it may be of benefit for the treatment of glaucoma. The mode of action is thought to be through prevention of damage to retinal ganglion cells as a result of increased intraocular pressure (27,28).

Memantine is a primary amine (pK_a 10.42) and is relatively lipophilic (log P 3.28). Hence, the physicochemical properties of memantine suggest that it may bind to ocular melanin through ionic interactions of its basic primary amine group. The high partition coefficient implies that there would be a good permeability of memantine through biologic membranes and, consequently, access to membrane-bound melanin. This would be expected to affect the drug's ocular pharmacokinetics. The objective of this work was to characterize the binding of memantine to different melanins. An understanding of the binding affinity and parameters of memantine to melanin are requisite for a complete understanding of its ocular disposition. Additionally, the affinity of memantine for melanin may yield further insight into the drug's vitreoretinal pharmacokinetics.

For this study three sources of melanin were used, sepia, synthetic, and bovine melanin, of which the latter was isolated from fresh specimens. Synthetic melanin is protein-free, whereas sepia and bovine melanin are conjugated to protein (12) and of invertebrate and mammalian origin, respectively. All sources of melanin were characterized by means of particle size and infrared spectroscopy. For the determination of the binding characteristics of memantine to melanin, deionized water and PBS were used as incubation media. Because melanin is virtually insoluble in aqueous solutions, the free memantine was separated from the melanin–memantine complex by centrifugation and subsequent filtration. The unbound fraction was then assayed and quantified using a validated LC–MS method (29), and from these data the binding parameters of memantine to melanin were determined.

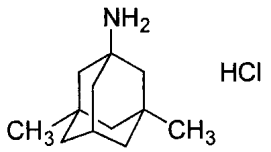

Fig. 1. Structure of memantine hydrochloride. Molecular formula $C_{12}H_{21}N{\cdot}HCl$; molecular weight 215.76 (free base 179.20); partition coefficient, log(P) 3.28; pK_a 10.42; solubility of the hydrochloride salt 3.5% in a pH 6.5 aqueous solution.

MATERIALS AND METHODS

Chemicals and Reagents

Memantine hydrochloride was obtained from Merz & Co. (Frankfurt, Germany). Melanin sepia officinalis, melanin synthetic (by oxidation of tyrosine with hydrogen peroxide), and formic acid were purchased from Sigma–Aldrich (St. Louis, MO). Potassium bromide was purchased from BDH (Poole, UK). Potassium phosphate monobasic was purchased from EM Science (Gibbstown, NJ). Sodium chloride and sodium phosphate dibasic heptahydrate were provided by Allergan (Irvine, CA). Phosphoric acid (85%) and sodium hydroxide (50% w/w) were purchased from Mallinckrodt–Baker (Phillipsburg, NJ). Methanol was of HPLC grade and obtained from Burdick & Jackson (Muskegon, MI). Deionized water was obtained from a Milli–Q system, Millipore (Bedford, MA, USA).

Instrumentation

Bovine tissues were homogenized using a Tissue Tearor (Model 985–370 Type 2, Biospec Products, Bartlesville, OK). Bovine melanin was purified using an Accuspin centrifuge (Beckman–Coulter, Fullerton, CA) and lyophilized with a Lyph Lock 6L Freeze Dry System (Model 77530, Labconco, Kansas City, MO).

The melanin particle size was determined with an LS230 Particle Sizer (Beckman–Coulter) with the small sample volume attachment and instrument performance test was ensured using Standard LS300 (Beckman–Coulter).

Fourier transform infrared (FT–IR) spectra were recorded on an Avatar 380 FT–IR spectrometer (Thermo–Nicolet, Madison, WI) fitted with the Avatar Diffuse Reflectance Smart accessory and operated by Thermo–Nicolet OMNIC software.

Melanin binding samples were incubated using an Environ–shaker from Lab Line Instruments (Melrose Park, IL). Separation of the melanin–memantine complex from the unbound memantine fraction was accomplished with a Baxter Biofuge A (Deerfield, IL).

LC–MS analyses were performed with a HP 1100 Series HPLC system connected to a HP 1100 MSD mass spectrometer both from Agilent Technologies (Palo Alto, CA). Data acquisition and integration was controlled by Agilent Technologies ChemStation software.

Buffer solution pH values were measured with a Beckman–Coulter Φ10 pH Meter, calibrated before use with Beckman–Coulter pH standard buffer solutions of pH 4 and 7.

Isolation of Bovine Melanin

Melanin was isolated from the iris, ciliary body, RPE, and choroid of bovine eyes (Sierra Medical Sciences, Santa Fe Springs, CA). The eyes were dissected on the same day of enucleation. Preceding homogenization the tissues were cut into smaller pieces. Deionized water was added, and the tissue was homogenized at speed 4 for 7 min in an ice/water bath. The homogenate was then centrifuged at 100 × *g* for 8 min, and the brown supernatant was retained. The pellet was resuspended in deionized water, homogenized at speed 4 for 2 min, and centrifuged at 100 × *g* for 8 min. This procedure was repeated until the pellet was gray and the supernatant

faint brown. The combined supernatant was then centrifuged at 350 × *g* for 15 min, the brown supernatant retained, the pellet resuspended in deionized water, homogenized at speed 4 for 2 min, and centrifuged at 350 × *g* for 15 min. This procedure was repeated until the pellet was gray and the supernatant faint brown. The combined supernatant was then centrifuged at 2780 × *g* for 20 min, retaining the dark brown pellet and discarding the supernatant. The melanin pellet was washed five times by repeated suspension in deionized water and centrifugation at 2780 × *g* for 20 min. Before lyophilization the melanin pellet was frozen at –20°C. The dried melanin was milled and stored for further use in an amber vial at –20°C.

Phosphate-Buffered Saline

Phosphate-buffered saline prepared in deionized water contained sodium chloride (154 mM), potassium phosphate monobasic (1.5 mM), and sodium phosphate dibasic (8.5 mM). The pH of the buffer was adjusted to 7.4 using either sodium hydroxide or phosphoric acid.

Characterization of Sepia, Synthetic, and Bovine Melanin

Particle Size Distribution

Separate suspensions (2.0 mg/ml) of sepia, synthetic, and bovine melanin were prepared in deionized water and PBS, followed by sonication for 15 min. Appropriate performance of the particle sizer was verified by the analysis of a control sample before analysis of samples, and all measurements were made against deionized water. Samples were analyzed in duplicate.

For the measurement of particle size the melanin suspension was added until polarization intensity differential scattering (PIDS) obscuration was between 45% and 55%. The Fraunhofer optical model including PIDS was used for the particle size measurement in the range of 0.04 to 2000 μm.

Fourier Transform Infrared Spectra

Samples for infrared analysis were prepared in the same way as samples for the determination of melanin–memantine binding parameters. Samples were prepared in deionized water and PBS by mixing equal volumes (1.0 ml) of melanin suspension (2.0 mg/ml) and memantine HCl solution (1000 μM). Controls for every melanin type and suspension fluid were prepared by incubating melanin suspension with the respective solvent. After incubation and centrifugation, the supernatant was decanted, and the pellet lyophilized. Test and control samples were prepared in triplicate.

A quantity (0.7 mg) of the lyophilized samples was mixed with potassium bromide (600 mg) and lightly ground in a mortar. The mixture was then placed into the instrument, and 64 scans in diffuse reflectance mode were collected for each spectrum. The background was measured using potassium bromide. All measurements were performed at room temperature and 4 cm^{-1} resolution.

Binding of Memantine to Melanin

Silanized glassware was used to minimize memantine surface adsorption. Memantine hydrochloride solutions were stored at room temperature for a maximum of 3 days.

Suspensions (2.0 mg/ml) of sepia, synthetic, and bovine melanin were prepared in deionized water and PBS, sonicated for 15 min, and warmed up to 37°C before incubation with memantine hydrochloride. While being stirred the melanin suspension (1.0 ml) was transferred into an incubation container (5 ml, polypropylene, VWR, San Diego, CA) and mixed with a memantine hydrochloride solution (1.0 ml) of the corresponding solvent.

To improve sample homogeneity the containers were placed horizontally in the temperature-controlled shaker, set to 37°C and 100 rpm. Samples for the binding study were prepared in triplicate. Controls were prepared by incubating memantine hydrochloride solution separately with deionized water or PBS. Also, controls were prepared by incubating each melanin suspension separately with deionized water and PBS.

The kinetics of the binding process was determined with memantine hydrochloride solutions (1500 nM) and various incubation times (10, 20, 30, 45, 60, and 90 min). The maximum binding capacity and dissociation constant were determined with memantine hydrochloride solutions in the concentration range 0.1 to 1000 μM (n = 13) and 90 min incubation time.

After incubation a portion of the sample was transferred into a centrifuge tube (Flex–Tube 1.5 ml, polypropylene, Eppendorf, Hamburg, Germany) and centrifuged at 14,900 × *g* for 15 min. The supernatant was drawn into a syringe and filtered through a nylon syringe filter (Nylon Acrodisc, 0.2 μm pore size, 25 mm membrane diameter, Gelman Sciences, Ann Arbor, MI). The first 0.5–0.6 ml of the filtrate was discarded, and the remaining volume filtered directly into an HPLC vial (0.75 ml, polypropylene, VWR, San Diego, CA), vortexed, and analyzed. Previous studies have shown that 0.5 ml was sufficient to saturate any filter sorption and eliminate any potential filter leachables.

Analytic Conditions

HPLC separations were carried out on a Prodigy ODS(3) column (100 × 4.6 mm, 5 μm particle size, 100 Å pore size) from Phenomenex (Torrance, CA). Mobile phases A and B were 0.1% (v/v) of formic acid in deionized water and 0.1% (v/v) of formic acid in methanol, respectively. The mobile phases were filtered through a 0.45-μm Nylaflo nylon membrane filter (Gelman Sciences) before use.

Gradient elution was used for the chromatographic separation of the analyte. The ratio of mobile phase A and B at the start of the analysis was 50% A and 50% B. The fraction of mobile phase B was then increased to 70% using a linear gradient for 3 min, which was followed with an isocratic period for 2 min. Over the following 0.5 min a linear gradient was used to restore the mobile phase ratio to the initial conditions, which were retained for a further 3.5 min. In all experiments the injection volume was 100 μl with a mobile phase flow rate of 0.8 ml/min. The autosampler and column were not temperature controlled.

Mass spectrometric detection was accomplished by splitless positive electrospray ionization at atmospheric pressure. The flow of the drying gas was set to 13.0 L/min at a temperature of 300°C. The nebulizer pressure was 206.8 kPa (30 psi). The capillary entrance and exit voltages were 3500 V and 70 V, respectively. Detection was performed in single ion

monitoring mode (m/z 180). The electron multiplier was set to 10,000 V with a gain of 1.0 and a dwell time of 580 ms and ion width of 0.05 m/z.

Quantification

Minitab 13 (State College, PA) was used to generate calibration curves by linear regression of peak area to memantine hydrochloride concentration with the use of a weighting factor of $1/x^2$ (where x is the concentration of memantine hydrochloride). Samples were bracketed by sets of four standard solutions.

Calculation of Binding Parameters

The calculation of binding parameters is based on the Langmuir binding isotherm, which assumes that receptor (R, melanin) and ligand (L, memantine) are in equilibrium with the receptor–ligand complex (RL, melanin–memantine complex). The equilibrium dissociation constant, K_D, is defined as the ratio of the rate constants and is identical to the ratio of the concentration of reactants and formed complex [Eq. (1)]. For practical reasons the affinity between receptor and ligand is usually described by the systems dissociation constant, K_D.

$$K_D = \frac{k_{-1}}{k_{+1}} = \frac{[R][L]}{[RL]} \quad (1)$$

where k_{+1} and k_{-1} are the reactions' association and dissociation constants, respectively.

The maximum amount of ligand bound to the receptor is commonly called B_{Lmax}. Correspondingly, the amount of ligand bound to the receptor at any ligand concentration is generally called B_L and equals $[RL]$ which gives the Langmuir binding isotherm [Eq. (2)].

$$B_L = \frac{B_{L\,\max}[L]}{K_D + [L]} \quad (2)$$

In Eq. (2), B_L (melanin–memantine binding) and $[L]$ (added memantine) are obtained experimentally, but B_{Lmax} and K_D remain to be determined. There are several approaches to obtaining these remaining parameters from the experimental data of which curve fitting is the most accurate.

Although it is thought that melanin has several classes of binding sites, the data were fit to one binding site. The randomness of the polymer and thus the unpredictability of the different modes of interaction involved in the binding process between memantine and melanin make the determination of the number of binding classes very difficult. Hence, the simplest solution of a model of one binding site was used which then was verified for validity by analysis of the curve fitting residuals for Gaussian distribution. Prism 2 (GraphPad Software, San Diego, CA) was used for the determination of the binding parameters.

RESULTS

Particle Size Distribution

Results of the particle size measurements are shown in Fig. 2 as a relative percentage frequency plot. The suspension medium had no effect on the particle size distribution of sepia melanin. Though the size of the particles ranged from 0.06 to 52 μm with a mode at 12.4 μm and a standard deviation (SD) of 7.1 μm, the particles between 0.06 and 2 μm were less than 5% of the total volume.

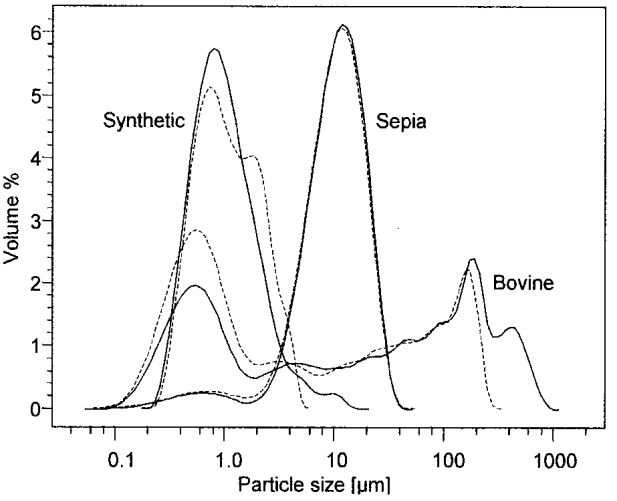

Fig. 2. Relative percentage frequency distribution of sepia, synthetic, and bovine melanin suspended in deionized water (solid lines) and PBS (dashed lines).

Synthetic melanin showed considerable differences in particle size distribution with the different two suspension media. When suspended in deionized water the particle size distribution was relatively unimodal between 0.2 and 19 μm with the mode at 0.8 μm and a SD of 1.5 μm, whereas in PBS it was bimodal and ranged from 0.2 to 6 μm with the first mode at 0.8 μm and a SD of 1.0 μm, and a minor second mode at 1.9 μm.

The particle size distributions of bovine melanin were similar in both suspension media up to 200 μm. Suspended in deionized water the particles ranged from 0.06 to 1150 μm with three modes at 0.5, 195, and 440 μm. In PBS the particle size was between 0.07 and 310 μm with two modes at 0.5 and 160 μm.

Fourier Transform Infrared Spectra

Samples obtained from both suspension media, deionized water and PBS, showed no differences in the FT–IR spectra between controls and samples that contained memantine. Compared to preparations obtained from deionized water was the band in the region of 1600 cm^{-1} accentuated in the preparations obtained from PBS.

There are differences between the FT–IR spectra of the controls, prepared in deionized water, of sepia melanin and those of synthetic and bovine melanin (Fig. 3) in the region of 3600 cm^{-1} and 2900 cm^{-1}, the low absorbance at 1750 cm^{-1}, and the low absorbance at around 1200 cm^{-1}. There are some minor differences when the spectrum of synthetic melanin is compared with that for bovine melanin. The spectrum of synthetic melanin in contrast to the one for bovine melanin had a shoulder at 2500 cm^{-1} with peak splitting at around 1700 cm^{-1} and a higher absorbance at around 950 cm^{-1}.

It is extremely difficult to assign the bands as it is thought that there are contributions from differences in hydration, protein conjugation, and the chemistry of the melanin polymer such as the DHI/DHICA ratio. Further, the presence of metal ions in melanin can produce spectral changes (30,31).

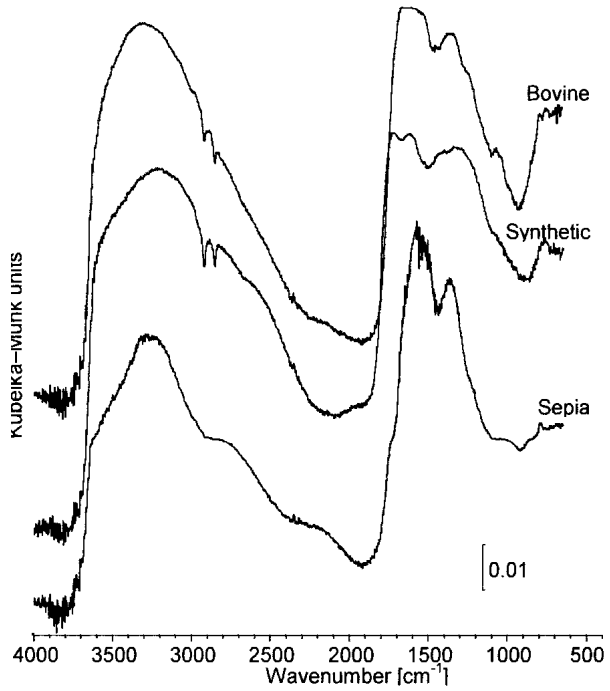

Fig. 3. FT–IR spectra recorded in diffuse reflectance mode of sepia, synthetic, and bovine melanin controls prepared in deionized water.

Binding of Memantine to Melanin

Binding Kinetics

For all the melanins and incubation media the melanin–memantine binding process appeared to occur virtually instantly, as the binding remained constant after an incubation time of 10 min (Fig. 4).

Differences in the amount of melanin–memantine binding depending on the melanin type and incubation medium are also illustrated in Fig. 4. In deionized water sepia and bovine melanin bound about 97% of the available memantine, and synthetic melanin bound about 70%. However, when incubated in PBS the binding characteristics were significantly different: sepia melanin bound about 59%, synthetic about 41%, and bovine bound about 30%.

Binding Capacity and Affinity

Results of the binding of various concentrations of memantine hydrochloride to sepia, synthetic, and bovine melanin suspended in deionized water and PBS are shown in Figs. 5 and 6. Experimental variations for the three melanins prepared with different concentrations of memantine hydrochloride were small for each melanin type and incubation medium.

The plateaus in the semilogarithmic plots (Fig. 5) of the binding of memantine to the different melanins vs. the concentration of memantine hydrochloride shows that near saturation has been approached and that the extent of binding was reduced in PBS. A logarithmic plot of the binding data (Fig. 6) shows an initial linear relationship between added memantine hydrochloride and binding for all the melanins up to a concentration of 5 and 50 μM for PBS and deionized water, respectively.

Results of the nonlinear regression of the binding data to the Langmuir binding isotherm for one binding site are shown in Figs. 7 and 8 and are summarized in Table I. Residuals of the curve-fitting analysis showed Gaussian distribution ($p > 0.1$), indicating that a one-site binding system may be a valid hypothesis.

Comparison of the results for the two suspension media shows that with PBS there was a reduced binding capacity for all the melanins, though the reduction was selective (Fig. 8). Sepia melanin in deionized water showed the greatest binding capacity for memantine, followed by bovine and synthetic melanin. In PBS, however, the rank order changed, and bovine melanin had the greatest binding capacity followed by sepia and synthetic melanin. Sepia melanin, which had the greatest binding capacity, also showed the largest reduction (~70%) caused by the buffer electrolytes; the reduction was a little less for synthetic melanin (~60%). For bovine melanin the presence of buffer electrolytes led to the lowest reduction of binding capacity (~40%).

Affinity (Fig. 8) of sepia and synthetic melanin for

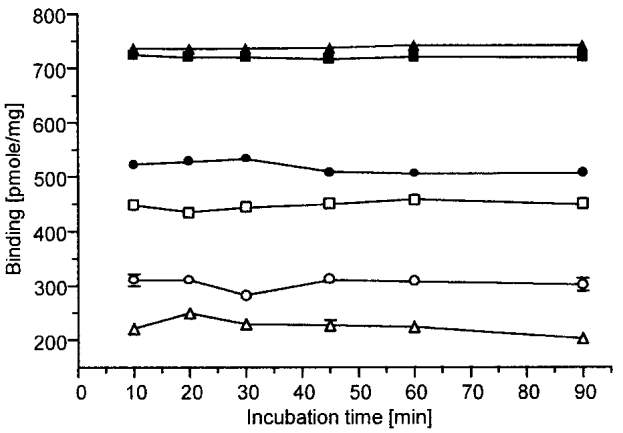

Fig. 4. Binding of memantine hydrochloride to sepia (squares), synthetic (circles), and bovine (triangles) melanin in deionized water (full symbols) and PBS (open symbols) after various incubation times. Error bars indicate standard deviation of three measurements and are generally encompassed by the symbol.

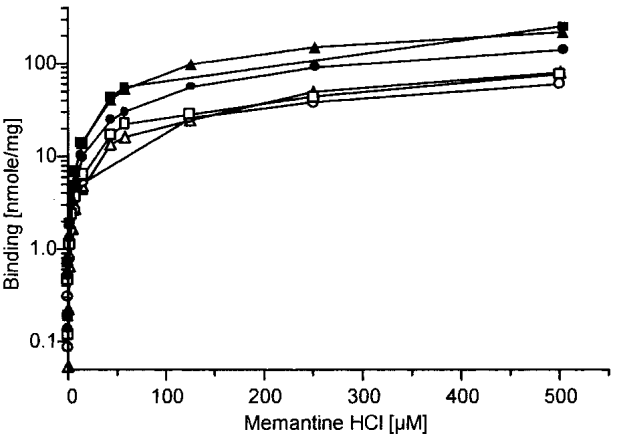

Fig. 5. Binding of memantine hydrochloride to sepia (squares), synthetic (circles), and bovine (triangles) melanin in deionized water (full symbols) and PBS (open symbols) at various concentrations of memantine hydrochloride. Error bars indicate standard deviation of three measurements and are generally encompassed by the symbol.

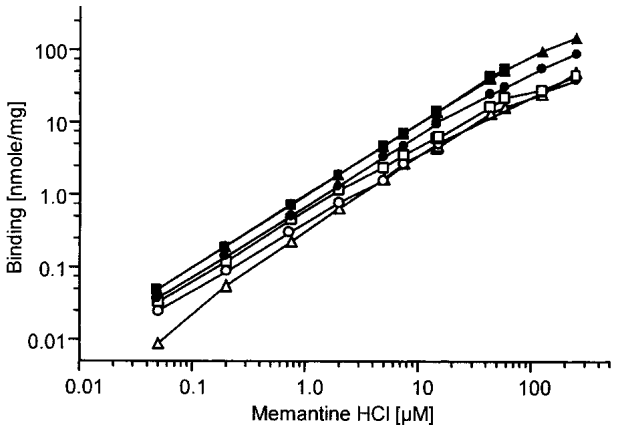

Fig. 6. Binding of memantine hydrochloride to sepia (squares), synthetic (circles) and bovine (triangles) melanin in deionized water (full symbols) and PBS (open symbols) at various concentrations of memantine hydrochloride. Error bars indicate standard deviation of three measurements and are generally encompassed by the symbol.

memantine was similar for both sources and remained largely unaffected by the suspension media. In deionized water, bovine melanin showed a smaller affinity for memantine than sepia and synthetic melanin but a greater affinity when suspended in PBS.

DISCUSSION

Bovine melanin was successfully isolated from melanin-containing ocular tissues (iris, ciliary body, RPE, and choroid) and lyophilized to obtain a homogeneous pigment.

Interpretation of the particle size data for the different melanins suspended in deionized water and PBS was complex, as the suspensions differed significantly in their size distribution. As a result of the nonhomogeneity of the size distribution, the use of general descriptors (i.e., mean, standard deviation, median, and mode) was limited and had to be more illustrative.

Although the suspensions of synthetic and sepia melanin in deionized water and PBS had a relatively narrow particle size distribution, bovine melanin showed a more complex, multimodal size distribution. The particle sizes of synthetic and sepia melanin can be characterized by their modes and standard deviations, but bovine melanin is more heterogeneous, with particle size ranging over several magnitudes with multiple modes. The reason for the different size distributions of synthetic and bovine melanin depending on the suspension media can only be speculative. The breakup of large agglomerates of bovine melanin in suspension may result from increased tensions within charge-transfer complexes formed between the melanin polymer and buffer ions. For synthetic melanin, the presence of buffer ions may assist further aggregation of small particles because of a different DHI/DHICA ratio of the oligomers compared to the natural melanins, where different processes may be involved in aggregation (8). This supposition is supported by the facts that synthetic melanin suspended in PBS had a greater population of larger particles and that the larger particles of bovine melanin present in deionized water disappeared when suspended in PBS as the population of smaller ones increased. Also, sepia melanin contains calcium and magnesium ions on isolation (32), which may explain a lack of the effect of electrolytes in the suspension media.

The different melanins were distinguishable by infrared analysis. However, a comprehensive elucidation of the spectral characteristics was difficult because of their complex nature. Although the underlying chemistry of the melanin sources is the main factor determining their infrared spectral properties, the degree of hydration and extent of protein conjugation may also contribute.

The binding of memantine to the different melanins was rapid, reaching equilibrium within an incubation time of 10 min.

In deionized water, sepia melanin had the highest binding capacity for memantine, followed by bovine and synthetic melanin. When measured in PBS, the binding capacity of all three melanins was lower than in deionized water, and the decrease was selective as the rank order had changed. When suspended in PBS, bovine melanin had the highest binding capacity, followed by sepia and synthetic melanin. This indicates that binding capacity is strongly and selectively influenced by the presence of electrolyte, which is suggestive of selective alterations in the binding sites on the melanin polymer. This overall reduction in binding capacity may be the

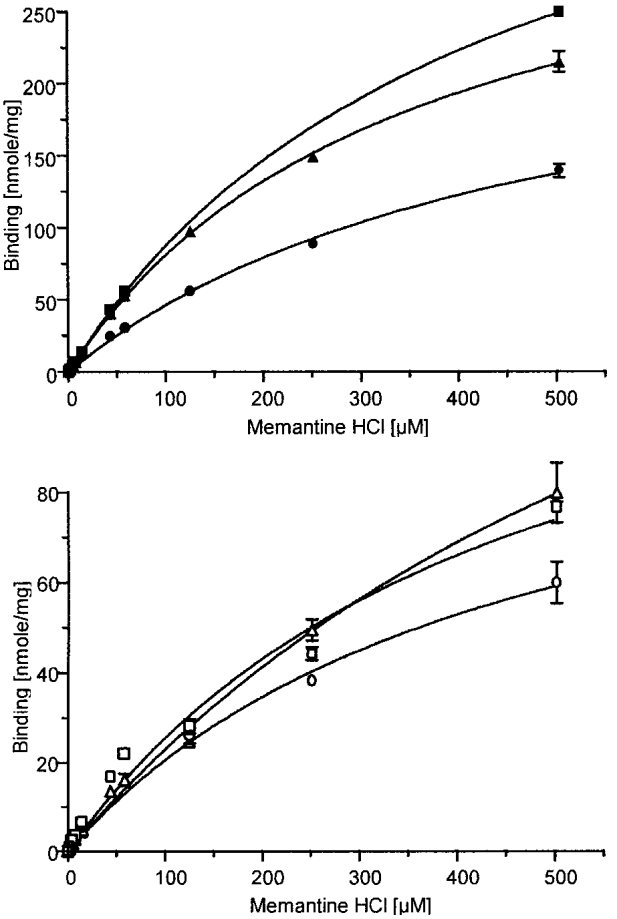

Fig. 7. Binding of memantine hydrochloride to sepia (squares), synthetic (circles) and bovine (triangles) melanin in deionized water (full symbols) and PBS (open symbols). Curves were obtained by nonlinear regression according to the Langmuir binding isotherm. Error bars indicate the standard deviation of three measurements and are generally encompassed by the symbol.

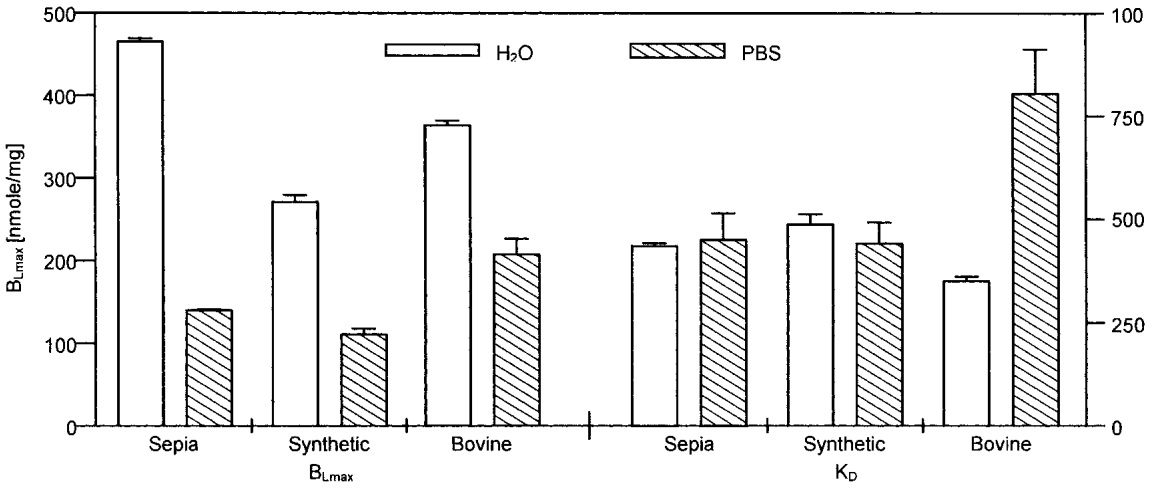

Fig. 8. Maximum binding capacity *(B_{Lmax})* and dissociation constant *(K_D)* of sepia, synthetic, and bovine melanin for memantine hydrochloride in deionized water (H_2O) and PBS. Error bars indicate the standard error.

result of competition between buffer ions and memantine for binding sites on the melanin polymer or a reduction in the ζ-potential or a combination of both. A reduction in ζ-potential could reduce electrostatic interactions.

The comparatively low binding capacity of synthetic melanin for memantine may be caused by a high DHI/DHICA ratio of the basic oligomer as fewer carboxylic acid groups imply that fewer binding sites are available. The dissociation constant of synthetic melanin, which remained unaffected by the suspension media, supports this hypothesis as the binding process of this melanin is thought to be primarily determined by its chemistry.

In contrast to synthetic melanin, it appears that the DHI/DHICA ratio for sepia and bovine melanin are considerably lower (9), as indicated by their increased binding capacity. However, a differing amount of protein bound to pigment, which is thought not to contribute to the binding process, may account for the observed differences in the binding capacities when suspended in deionized water. Furthermore, the breakdown of bovine melanin agglomerates into smaller ones when suspended in PBS may expose additional and more easily accessible binding sites. Hence, bovine melanin suspended in PBS shows a relatively small decrease in binding capacity because of competition of memantine with buffer ions but a greater increase in binding affinity because of more accessible binding sites.

Kristensen *et al.* (17) investigated the binding of antimalarial drugs such as chloroquine and quinine to sepia melanin suspended in phosphate buffer and obtained binding capacities that were, respectively, seven and four times higher than for memantine. The dissociation constants were about twice as high for both compounds. Schoenwald *et al.* (16) determined the binding characteristics of carbonic anhydrase inhibitors such as methazolamide and a sulfonamide to sepia melanin in phosphate buffer. The respective binding capacities for these drugs were about 1.4 and 3.3 times higher than for memantine; the respective dissociation constants, however, were seven and ten times lower than of memantine. In

Table I. Nonlinear Regression of Binding Data to the Langmuir Binding Isotherm

	Deionized water			PBS		
	Sepia	Synthetic	Bovine	Sepia	Synthetic	Bovine
Best-fit values						
B_{Lmax} (nmol/mg)	466	272	364	140	111	207
(SE)‡	(4)	(8)	(5)	(12)	(7)	(19)
K_D (μM)	435	488	351	452	442	804
(SE)	(7)	(25)	(10)	(63)	(52)	(108)
95% Confidence intervals						
B_{Lmax} (nmol/mg)	458 to 473	255 to 288	353 to 375	117 to 164	96.1 to 126	168 to 246
K_D (μM)	422 to 449	438 to 538	332 to 371	323 to 580	335 to 548	586 to 1020
Goodness of fit						
Degrees of freedom	31	37	37	37	27	36
R^2*	1.00	0.998	0.999	0.981	0.993	0.991
Abs. Sum of Sq.†	1.994×10^7	1.426×10^8	1.408×10^8	3.446×10^8	7.819×10^7	1.801×10^8
Sy.x§	802	1960	1950	3050	1700	2240

‡ SE, standard error.
* Goodness-of-fit.
† Absolute sum of squares.
§ Standard deviation of the vertical distances of the points from the line.

another study when the binding properties of sympathomimetic amines to synthetic L-dopa melanin in phosphate buffer were investigated (12), amphetamine, ephedrine, octopamine, and cocaine all bound over 30 times less with dissociation constants over 4×10^4 times lower than for memantine.

This study showed that sepia, synthetic, and bovine melanin differ significantly in their particle sizes, infrared spectra, and binding characteristics. These differences among the investigated melanins were thought not only to be primarily caused by differences in melanin chemistry such as the DHI/DHICA ratios and protein conjugation but also by the incubation medium. For a correlation of results of *in vitro* drug–melanin binding experiments to the drugs' ocular pharmacokinetics, the results of this study also indicate the significance of using the appropriate source of melanin.

ACKNOWLEDGMENTS

This study was supported by grants from Allergan Inc., Irvine, CA. M.J.K. also gratefully acknowledges the opportunity to undertake this study at Allergan Inc.

REFERENCES

1. R. M. J. Ings. The melanin binding of drugs and its implications. *Drug Metab. Rev.* **15**:1183–1212 (1984).
2. G. Prota. *Melanins and Melanogenesis*. Academic Press, London, 1992.
3. S. E. Forest and J. D. Simon. Wavelength-dependent photoacoustic calorimetry study of melanin. *Photochem. Photobiol.* **68**:296–298 (1998).
4. U. Schraermeyer, S. Peters, G. Thumann, N. Kociok, and K. Heimann. Melanin granules of retinal pigment epithelium are connected with the lysosomal degradation pathway. *Exp. Eye Res.* **68**:237–245 (1999).
5. U. Schraermeyer and K. Heimann. Current understanding on the role of retinal pigment epithelium and its pigmentation. *Pigm. Cell Res.* **12**:219–236 (1999).
6. T. Sarna. Properties and function of the ocular melanin—a photobiophysical view. *J. Photoch. Photobio. B.* **12**:215–258 (1992).
7. C. M. R. Clancy and J. D. Simon. Ultrastructural organization of eumelanin from *Sepia officinalis* measured by atomic force microscopy. *Biochemistry-US* **40**:13353–13360 (2001).
8. J. B. Nofsinger, S. E. Forest, L. M. Eibest, K. A. Gold, and J. D. Simon. Probing the building blocks of eumelanins using scanning electron microscopy. *Pigm. Cell Res.* **13**:179–184 (2000).
9. A. Pezzella, M. D'Ischia, A. Napolitano, A. Palumbo, and G. Prota. An integrated approach to the structure of sepia melanin. evidence for a high proportion of degraded 5,6-dihydroxyindole-2-carboxylic acid units in the pigment backbone. *Tetrahedron* **53**: 8281–8286 (1997).
10. L. Novellino, A. Napolitano, and G. Prota. Isolation and characterization of mammalian eumelanins from hair and irides. *Biochim. Biophys. Acta* **1475**:295–306 (2000).
11. M. Olivieri and R. A. Nicolaus. On the structure of DHI-melanin, *Rend. Acc. Sci. Fis. Mat.* Vol. LXVI, (1999), http://www.tightrope.it/nicolaus/11b.htm.
12. M. M. Salazar-Bookaman, I. W. Wainer, and P. N. Patil. Relevance of drug-melanin interactions to ocular pharmacology and toxicology. *J. Ocul. Pharmacol.* **10**:217–239 (1994).
13. J. M. Gallas, G. W. Zajac, T. Sarna, and P. L. Stotter. Structural differences in unbleached and mildly-bleached synthetic tyrosine-derived melanins identified by scanning probe microscopies. *Pigm. Cell Res.* **13**:99–108 (2000).
14. G. W. Zajac, J. M. Gallas, J. Cheng, M. Eisner, S. C. Moss, and A. E. Alvarado-Swaisgood. The fundamental unit of synthetic melanin: a verification by tunneling microscopy of X-ray scattering results. *Biochim. Biophys. Acta* **1199**:271–278 (1994).
15. C. M. R. Clancy, J. B. Nofsinger, R. K. Hanks, and J. D. Simon. A hierarchical self-assembly of eumelanin. *J. Phys. Chem. B* **104**: 7871–7873 (2000).
16. R. D. Schoenwald, V. Tandon, D. E. Wurster, and C. F. Barfknecht. Significance of melanin binding and metabolism in the activity of 5-acetoxyacetylimino-4-methyl-delta(2)-1,3,4,-thiadiazoline-2-sulfonamide. *Eur. J. Pharm. Biopharm.* **46**:39–50 (1998).
17. S. Kristensen, A. L. Orsteen, S. A. Sande, and H. H. Tonnesen. Photoreactivity of biologically-active compounds VII. interaction of antimalarial-drugs with melanin *in-vitro* as part of phototoxicity screening. *J. Photochem. Photobiol. B.* **26**:87–95 (1994).
18. S. Persad, J. D. Wiltshire, I. A. Menon, P. K. Basu, and F. Carre. Role of melanin in drug accumulation in the eye and ocular toxic reaction. *J. Invest. Dermatol.* **87**:432 (1986).
19. B. Leblanc, S. Jezequel, T. Davies, G. Hanton, and C. Taradach. Binding of drugs to eye melanin is not predictive of ocular toxicity. *Regul. Toxicol. Pharmacol.* **28**:124–132 (1998).
20. A. M. Potts. The reaction of uveal pigment *in vitro* with polycyclic compounds. *Invest. Ophth. Visual* **3**:405–416 (1964).
21. P. R. Raghavan, P. A. Zane, and S. L. Tripp. Calculation of drug-melanin binding energy using molecular modeling. *Experientia* **46**:77–80 (1990).
22. A. H. Lowrey, G. R. Famini, V. P. Loumbev, L. Y. Wilson, and J. M. Tosk. Modeling drug-melanin interaction with theoretical linear solvation energy relationships. *Pigm. Cell Res.* **10**:251–256 (1997).
23. B. S. Larsson. Interaction between chemicals and melanin. *Pigm. Cell Res.* **6**:127–133 (1993).
24. I. A. Menon, G. E. Trope, P. K. Basu, D. C. Wakeham, and S. D. Persad. Binding of timolol to iris-ciliary body and melanin: an *in vitro* model for assessing the kinetics and efficacy of long-acting antiglaucoma drugs. *J. Ocul. Pharmacol.* **5**:313–324 (1989).
25. B. Larsson and H. Tjälve. Studies on the mechanism of drug-binding to melanin. *Biochem. Pharmacol.* **28**:1181–1187 (1978).
26. H. S. V. Chen, J. W. Pellegrini, S. K. Aggarwal, S. Z. Lei, S. Warach, F. E. Jensen, and S. A. Lipton. Open-channel block of N-methyl-D-aspartate (NMDA) responses by memantine—therapeutic advantage against NMDA receptor-mediated neurotoxicity. *J. Neurosci.* **12**:4427–4436 (1992).
27. W. A. Lagreze, R. Knorle, M. Bach, and T. J. Feuerstein. Memantine is neuroprotective in a rat model of pressure-induced retinal ischemia. *Invest. Ophth. Vis. Sci.* **39**:1063–1066 (1998).
28. C. K. Vorwerk, S. A. Lipton, D. Zurakowski, B. T. Hyman, B. A. Sabel, and E. B. Dreyer. Chronic low-dose glutamate is toxic to retinal ganglion cells—toxicity blocked by memantine. *Invest. Ophth. Vis. Sci.* **37**:1618–1624 (1996).
29. M. J. Koeberle, P. M. Hughes, C. G. Wilson, and G. G. Skellern. Development of a liquid chromatography–mass spectrometric method for measuring the binding of memantine to different melanins. *J. Chromatogr. B* **787**:313–322 (2003).
30. K. B. Stepien, J. P. Dworzanski, B. Bilinska, M. Porebska-Budny, A. M. Hollek, and T. Wilczok. Catecholamine Melanins. Structural changes induced by copper ions. *Biochim. Biophys. Acta* **997**:49–54 (1989).
31. L. Bardani, M. G. Bridelli, M. Carbucichio, and P. R. Crippa. Comparative Mössbauer and infrared analysis of iron-containing melanins. *Biochim. Biophys. Acta* **716**:8–15 (1982).
32. R. A. Nicolaus and M. Piattelli. Structure of melanins and melanogenesis. *J. Polym. Sci.* **58**:1133–1139 (1962).